

Estimation-Aware Trajectory Optimization with Set-Valued Measurement Uncertainties

Aditya Deole ^{*} and Mehran Mesbahi [†]
University of Washington, Seattle, Washington, 98195-2400

In this paper, we present an optimization-based framework for generating estimation-aware trajectories in scenarios where measurement (output) uncertainties are state-dependent and set-valued. The framework leverages the concept of regularity for set-valued output maps. Specifically, we demonstrate that, for output-regular maps, one can utilize a set-valued observability measure that is concave with respect to finite-horizon state trajectories. By maximizing this measure, optimized estimation-aware trajectories can be designed for a broad class of systems, including those with locally linearized dynamics. To illustrate the effectiveness of the proposed approach, we provide a representative example in the context of trajectory planning for vision-based estimation. We present an estimation-aware trajectory for an uncooperative target-tracking problem that uses a machine learning (ML)-based estimation module on an ego-satellite.

Nomenclature

$x_k \in \mathbb{R}^{n_x}, u_k \in \mathbb{R}^{n_u}, y_k \in \mathbb{R}^{n_y}$	=	discrete time state, input and output triplet at time k
$\mathcal{E}(x, Q)$	=	ellipsoid centered at x with size $Q \in \mathbb{S}^+$
\mathcal{Y}_x	=	output set at state x
$\mathcal{X} \subset \mathbb{R}^{n_x}, \mathcal{U} \subset \mathbb{R}^{n_u}$	=	feasible state and input sets
$\Lambda(\mathcal{Y}_x)$	=	function defining maximum size of set \mathcal{Y}_x
$\ \cdot\ $	=	2-norm
A, B, C	=	state space system matrices
$d(\cdot, \cdot)$	=	distance metric
$x_{0:T}, u_{0:T}$	=	discrete state and input sequences from time 0 to T
$\Gamma_{x_0} u_{0:T-1}$	=	output tube mapped from initial state x_0 with an input sequence $u_{0:T}$
$Y_{x_{0:T}}$	=	output tube generated for state sequence from time 0 to T
$D_O(Y_{\bar{x}_{0:T}}), D_O^l(Y_{\bar{x}_{0:T}})$	=	Degree of observability and its lower bound

^{*}Ph.D. Candidate, Department of Aeronautics and Astronautics.

[†]Professor, Department of Aeronautics and Astronautics, AIAA Fellow.

I. INTRODUCTION

TRAJECTORY planning often involves solving optimization problems that minimize energy consumption while steering to a desired final state, ensuring that the system dynamics remain feasible under a set of constraints [1]. In this work, we examine a scenario where the planning problem must account for state estimation. This consideration is particularly relevant in safety-critical applications, where accurate state estimation is essential.

Traditionally, in offline planning, the estimation aspect is often neglected, potentially causing the trajectory to traverse regions with high measurement uncertainty. Larger measurement errors or disturbances directly lead to higher state estimation errors. Consequently, for some critical applications, estimation-aware trajectory design becomes indispensable [2]. State estimators map process measurements to full state estimates, provided the system is observable [3–7]. The performance of these estimators is closely tied to the quality of sensor measurements over time. If the sensor performance varies across states and time, visiting states where sensors have improved performance can enhance the corresponding state estimation. One common approach to redesign optimal trajectories for improved state estimation is to incorporate a secondary objective function into the original trajectory optimization problem [8, 9]. This augmented objective function must account for the quality of estimation with respect to the state vectors. Given knowledge of the uncertainty distribution, a suitable metric for capturing estimation quality can then be developed.

Deterministic systems with sensing uncertainties are often classified as partially observed stochastic dynamical systems. For these systems, estimation performance measures must be defined as an optimization objective. Conventionally, performance metrics for evaluating estimation include error probabilities [10], mean squared errors [11–13], Fisher information [14–16], entropy metrics and other belief state functions. For example, a commonly used construct in settings with Gaussian noise is the Fisher Information Matrix (FIM) [15, 16]. FIM is a metric that quantifies how much information about an unknown parameter is contained in a measurement. As such, FIM measures the amount of “information” on state x in the output measurement y . In the matrix case, the inverse of FIM provides the lower bound for the expected state estimate covariance, using the celebrated Cramer-Rao inequality [17, 18], i.e., $\mathbb{E}\{(\hat{x}-x)(\hat{x}-x)^T\} \geq \mathcal{I}^{-1}$, where \mathcal{I} denotes the FIM. This lower bound represents the covariance achieved by an unbiased estimator for the corresponding estimation problem. Therefore, for such an estimator, maximizing the determinant of the FIM over a trajectory improves the covariance performance of the state estimator. Other measures of the FIM, such as its spectral bounds, determinant, or trace, are also considered in various applications for estimation-aware planning [19].

The FIM metric utilized to quantify the information content of a measurement scheme are effective for parameter estimation when the underlying state is static. On the other hand, measures such as posterior FIM have been studied to analyze state estimation for Linear Time Invariant (LTI) systems [20, 21]. Optimization-based approaches demonstrate similar use of state covariance metrics for trajectory planning problems [22, 23].

Another framework for designing estimation-aware trajectories is to use observability-based metrics. Specifically, the Observability Gramian (OG) of a system, mapping initial conditions to an output trajectory sequence, can be used to

assess how sensitive state estimation is to perturbations in output measurements. Previous works in this direction have demonstrated that properties of the Empirical Gramian (EG) can be leveraged to improve conditioning for estimation process [24, 25]. These works show that using the EG generated from model prediction, an optimization problem can be formulated for generating a qualitatively more observable trajectory. These trajectories have improved estimation performance based on the type of metric used on the EG [8, 26–28]. These studies primarily focus on applications with deterministic output maps with Gaussian noise, that can be predicted forward, multiple roll-outs at a time. The computation of EG is also subject to the condition that deterministic measurements can be generated and predicted given an initial condition [29, 30]. In this work, we provide an alternative perspective that complements the existing frameworks, particularly for scenarios where measurements are set-valued and conventional method for EG computation is infeasible. But similar to EG-based approach, we use set distance metrics to generate a measure that improves conditioning of estimators over a trajectory.

Previous works in estimation-aware trajectory design primarily focus on deterministic output maps in the case of OG-based optimization or probabilistic models in the covariance-based optimization. Non-optimization based approaches often rely on pre-planning, using path-planning methods like Rapidly Exploring Random Trees (RRT) to find alternate, more estimation-aware trajectories. Some methods in the literature rely on application-specific correlations between estimation and the underlying state for trajectory design..

In our work, we present a framework for an optimization-based approach to trajectory design in scenarios where the output uncertainty is set-valued. In the domain of filtering on set-valued uncertainty, set-membership estimation has been investigated solely for the purpose of filtering where estimation procedures for set-based outputs are analyzed [31–33]. To the best of our knowledge there have not been any works on estimation-aware planning with set-based output uncertainties. The previous works on set-membership signify the need for a filtering method for cases where noise distributions are unknown but bounded. In our work, we specifically focus on measurement spaces with state-dependent uncertainties that are often non-Gaussian, as for example is the case in perception-aware planning. For such settings, we provide an explicit approach to estimation-aware planning for locally linearized systems.

The proposed approach is also applicable to nonlinear settings with invertible observability maps. Moreover, in our setup, we do not assume a specific distribution for the uncertainties within the set; however, we do impose a constraint that the corresponding uncertainty set is compact (i.e., closed and bounded in a finite-dimensional Euclidean space). Additionally, we assume that the “shape” of uncertainty set size is convex with respect to the state vector; this ensures an efficient solution strategy for the corresponding optimization problem. In subsequent parts of this paper, we will provide justifications for this assumption and discuss the potential conservatism that it introduces.

In our model, the output map is represented as a bounded set-valued uncertainty over a linear output measurement. Although convexity of this uncertainty is not always inherent in real-world applications, variations in uncertainty and its state dependence are often encountered in practice. In order to address such scenarios, we propose approximating the

uncertainty set using an enveloping convex function that provides an upper bound for this set. Using the convex output map (exact or approximate) we then proceed to construct a metric for observability that correlates with the estimation quality. We demonstrate that by maximizing this notion of observability, estimation performance improves. The observability metric is then introduced in §III as a convex surrogate for managing uncertainty, subsequently incorporated in a generic optimal trajectory design problem, as shown in §V.A.

Not that this work is an extension to [34] where we presented the pipeline for designing estimation aware trajectories using Nonlinear Model Predictive Control (N-MPC) using distinguishability based notions for set-based outputs. In our current work we are presenting a framework for establishing guarantees for existence of estimation aware trajectories. In this work we will show that a convex optimization problem can be set up to solve for the desired trajectory if certain conditions on output uncertainty sets can be established.

The paper is organized as follows: In §II, we define the system and outline the properties of the set-valued output uncertainty map. In §III, we introduce observability conditions and propose our primary criterion of finite horizon weak observability for set-valued maps. We then define a notion for a degree of observability, that serves as the evaluation metric for the planned trajectory. §IV presents our main results, where we discuss the convexity of the observability-based metric. Next, in §V, we formulate the optimization problem to compute a desired deviated trajectory that maximizes observability relative to a baseline nominal trajectory. Finally, in §V.A, we provide an example, and in §V.B, we showcase an application. In the satellite rendezvous example, we demonstrate that for a given nominal trajectory, an optimization problem can be solved to generate a deviated trajectory by maximizing the observability metric under state and input constraints. Additionally, we show that trajectory planning can be performed from scratch with the augmented observability term.

Notation: We denote the state vector for the system of interest at time t as x_t , and state vector dependent sets as \mathcal{Y}_{x_t} or $\mathcal{E}(\cdot)$ for set-valued maps. The maximum eigenvalue for a symmetric matrix is denoted by λ_{\max} and maximum and minimum singular values of the matrix A are denoted by σ_{\max} and σ_{\min} , respectively. The distance metrics used in the paper are follows: $d(a, b) = \|a - b\|$, where $\|\cdot\|$ is the Euclidean norm, $d_s(\cdot, \cdot)$ is the set distance (the infimum of the distance between a point and elements of the set), and $d_T(\cdot, \cdot)$ is the tube (sequence of sets) distance. State vector sequences are defined by $x_{0:T} = x_0, \dots, x_T$. Mappings from point-wise state x_0 , for a given input state sequence $u_{0:T-1}$, to set-valued sequence output are denoted as $\Gamma_{x_0} u_{0:T-1}$; occasionally, we also use an abbreviated notion Γ_{x_0} to denote this map. Norm balls with radius $\epsilon > 0$ are defined as $B_\epsilon(x_0) = \{x \mid \|x - x_0\| \leq \epsilon\}$.

II. Set-valued uncertainty model

We now formalize an observability metric that we will subsequently utilize to design estimation-aware trajectories. This metric is developed such that maximizing its lower bound improves observability of the state, hence improving measurement driven estimation. We will then show that this metric can be augmented to a conventional optimal

trajectory design problem for generating estimation-aware trajectories. The model that we consider for the trajectory planning problem is built upon the discrete time linear time invariant system of the form,

$$x_t^+ = Ax_t + Bu_t, \quad (1)$$

$$y_t = Cx_t + \varepsilon_t, \quad (2)$$

where $x_t \in \mathcal{X} \subset \mathbb{R}^{n_x}$ and $u_t \in \mathcal{U} \subset \mathbb{R}^{n_u}$ are feasible state and control inputs for $t = 0, 1, 2, \dots$, and ε_t is set-valued, as opposed to say, point-wise deterministic measurements or sampled from a known probability distribution such a Gaussian. The output at iteration t is modeled as a compact set, in the neighborhood of nominal output Cx_t . The set of possible deterministic outputs are defined as a state dependent set $\mathcal{Y}_x = Cx \oplus \mathcal{E}$, where “ \oplus ” denotes set-addition and \mathcal{E} denotes the measurement uncertainty set. This uncertainty captures all the deviations we might observe due to noise, disturbances or other unknown parameters that may affect such a measurement.

In this work, the measurement uncertainty is characterized by maximal ellipsoids, providing a convenient tie-in with the subsequent optimization setup. The maximal ellipsoid will bound the set-valued uncertainty observed in our model by a state dependent ellipsoid centered around the nominal linear measurement, $y = Cx$. An ellipsoidal set centered at x_0 is defined as,

$$\mathcal{E}(x_0, Q(x_0)) = \{x \mid (x - x_0)^\top [Q(x_0)]^{-1} (x - x_0) \leq 1\}, \quad (3)$$

where $Q(x_0) > 0$ (positive definite) and is dependent on x_0 ; we will adopt the notation $\mathcal{E}(x)$ for a generic ellipsoid centered at x . We use this ellipsoidal model to examine the output uncertainty map. Hence, for any state $x \in \mathcal{X}$, we have a point-to-set map defined by $\mathcal{Y}_x = \mathcal{E}(Cx, Q(Cx))$, where the output uncertainty ellipsoid is,

$$\mathcal{Y}_x := \mathcal{E}(y, Q(Cx)) = \{y \mid (y - \bar{y})^\top [Q(Cx)]^{-1} (y - \bar{y}) \leq 1\}. \quad (4)$$

The key problem implicit in our setup is addressing the selection of the input sequence (through the state dynamics), such that the state remains “distinguishable” throughout the trajectory. The notions of distinguishability for characterizing observability of a system were defined by Hermann and Krener [35] for general class of deterministic systems. In this work we, we modify these notions for designing a conservative notion of observability for set-based outputs. Here we must note that for our purpose the map of state to output uncertainty ellipsoids is known. Otherwise, it must be generated through a validation step in a simulation environment, as the metric we design relies on the knowledge of the corresponding uncertainty bounds. This assumption is similar to case where the probability distribution or error covariances for sensor’s uncertainty are known.

For our optimization approach to estimation-aware planning, a metric is needed to quantify the size of the uncertainty set. We adopt a conservative method for comparing ellipsoidal uncertainty sets based on their radii. Specifically, the maximum eigenvalue of the positive definite matrix defining the ellipsoid will be used as this metric.

Note that for any ellipsoid centered at x , the maximum distance from x to any other element in the ellipsoid is in fact the largest eigenvalue of the positive definite matrix defining the ellipsoid. Hence,

$$\sup_{y \in \mathcal{Y}_x} d(x, y) = \lambda_{\max}(Q_x); \quad (5)$$

we will use the notation $\Lambda(\mathcal{Y}_x)$ to define the map that generates the largest eigenvalue representing the size of the ellipsoidal uncertainty set corresponding to the state x . To put the setup into context, essentially a state x maps to the set \mathcal{Y}_x that represents the set of all possible outputs, and $\Lambda(\mathcal{Y}_x)$ characterizes the size of the image of this map.

Given this measure of the ellipsoidal uncertainty set at any point, we also need to quantify how this quantity varies spatially, that is, quantify the variation in its size with respect to x . A key assumption in our subsequent analysis is that the ellipsoidal measure, as a function of state x , is convex and bounded over a domain $\mathcal{S} \subset \mathcal{X}$.

Assumption II.1 *The largest eigenvalue of the output uncertainty ellipsoid defined by $\Lambda(\mathcal{Y}_x)$. The map Λ is convex and uniformly bounded for all $x \in \mathcal{S} \subset \mathcal{X}$.*

As convexity implies local boundedness of the error metric on any open subset of \mathcal{X} , a general result of Lipschitzness of $\Lambda(Q_x)$ also holds [36]. Thus we have,

$$|\Lambda(\mathcal{Y}_x) - \Lambda(\mathcal{Y}_{\bar{x}})| \leq L(\bar{x}) \|x - \bar{x}\|, \quad (6)$$

where $L(\bar{x})$ is the ‘‘local’’ variation Lipschitz parameter. This parameter can be written as

$$L(\bar{x}) = \frac{2M(\bar{x}, r)}{r}, \quad \text{where } M(\bar{x}, r) = \max_{x \in B_r(\bar{x})} \{\Lambda(x)\},$$

where M represents the local bound on $\Lambda(\bar{x})$. We can also see that $L(\bar{x})$ is convex with respect to \bar{x} .

As such from Eq. (6), we also have the inequality,

$$|\Lambda(\mathcal{Y}_x)| \leq |\Lambda(\mathcal{Y}_{\bar{x}})| + L(\bar{x}) \|x - \bar{x}\|. \quad (7)$$

Assumption II.1 and condition Eq. (7) provide enough control over maximum ellipsoidal uncertainty variation locally for every $x \in \mathcal{S}$.

A note on convexity of the output-map uncertainty

This work focuses on scenarios where the state dependence of output uncertainty can be distinctly quantified. The generation of estimation-aware trajectories becomes meaningful only if certain states improve state estimation relative to others. Conversely, if the uncertainty set is uniform over all states, estimation performance remains consistent, making trajectory optimization unnecessary. For cases with known state dependence, we aim to design an optimization problem that produces a unique exploration trajectory. In §III, we demonstrate that Assumption II.1 plays a crucial role in ensuring a unique solution.

In some applications, state dependence may not exhibit convexity but instead display local monotonicity that aids exploration. For example, quasi-convex functions, which have state-dependent uncertainties with a unique minimum, are relevant in such cases. This behavior is common in vision-based sensing, where identifiers or features are most visible at specific states, with sensing accuracy diminishing monotonically as one moves away from these optimal visibility states. To address such cases, we propose approximating the uncertainty size $\Lambda(Q)$ using an enveloping convex function, providing an algorithmically useful upper bound. This function is defined as $\hat{\Lambda}(x) = \inf\{g(x) | g \text{ is convex and } g \geq \Lambda\}$. The selection of candidate convex function g depends on the specific application*. Note that this approach results in an over-approximation of the upper bound. In subsequent analysis, we will use the notation Λ to refer to the envelope $\hat{\Lambda}$.

Using the enveloping function, we now compute the observability metric via a separation function. This separation function is a distance metric between sets, defined to be positive when distinguishing trajectories are generated from neighboring initial conditions. Finally, with the approximated convex upper bound on output uncertainty, the optimization approach described in §V can then be applied. In practical settings, designing the enveloping function from data is referred to as the validation procedure. For our case study on the Ego-Target problem, this validation procedure is detailed in §VII.B.

Set Distance metric

Thus far, we have explored methods for quantifying variations in the size of ellipsoidal uncertainty sets. For our observability analysis, we also need to define a metric for measuring the separation between these sets.

Definition II.1 (*Set Distance*) *The distance between two sets \mathcal{A} and \mathcal{B} in \mathcal{X} is defined as,*

$$d_s(\mathcal{A}, \mathcal{B}) = \inf \{d(v, w) \mid v \in \mathcal{A}, w \in \mathcal{B}\}. \quad (8)$$

Note that Eq. (8) is in fact a *pseudo-metric* on sets in \mathcal{X} , as $d_s(\mathcal{A}, \mathcal{B}) = 0$ does not imply $\mathcal{A} = \mathcal{B}$; instead this distance is zero when $\mathcal{A} \cap \mathcal{B} \neq \emptyset$.

*In the context of this work, we require the function g to only be convex. The convexity metric we derive from this function will be used as the objective function to an optimization problem. Therefore for faster convergence rates with gradient descent, we can select g to be strongly convex leading a linear rate of convergence (Polyak-Lojasiewicz (PL) inequality).

We now use the set distance to quantify how distinct output trajectories are for our setup. A lower bound on Eq. (8) can be computed if we consider the sets $\mathcal{E}(x_1)$ and $\mathcal{E}(x_2)$. Consider $v \in \mathcal{E}(x_1)$ and $w \in \mathcal{E}(x_2)$. Since,

$$d(x_2, v) \leq d(v, w) + d(w, x_2) \quad (9)$$

$$d(x_1, x_2) \leq d(x_1, v) + d(x_2, v) \quad (10)$$

it follows that $d(v, w) \geq d(x_1, x_2) - d(x_1, v) - d(w, x_2)$.

In our setting, the size of the uncertainty ellipsoids are comparatively small as compared with the distance between their respective centers; as such, substituting Eq. (9) into Eq. (10) we obtain,

$$d(v, w) \geq d(x_1, x_2) - d(x_1, v) - d(w, x_2) > 0 \quad (11)$$

where positivity constraint represents that sets do not intersect. Taking the infimum in Eq. (11), it now follows that,

$$\begin{aligned} \inf_{v,w} d(v, w) &\geq \inf_{v,w} \{d(x_1, x_2) - d(x_1, v) - d(w, x_2)\} \\ &\geq \max \{0, d(x_1, x_2) \} \end{aligned} \quad (12)$$

$$- \sup_v \{d(x_1, v)\} - \sup_w \{d(w, x_2)\} \}. \quad (13)$$

The lower bound on this set distance for maximal ellipsoids, is given by

$$\begin{aligned} d_s(\mathcal{E}(x_1), \mathcal{E}(x_2)) &\geq \max \{0, \|x_1 - x_2\|_2 \\ &\quad - |\Lambda(Q(x_1)) - \Lambda(Q(x_2))| \}. \end{aligned} \quad (14)$$

Here we have defined the set distance to be non-negative—hence, it behaves as a pseudo-metric. The lower bound on set distance function is derived by substituting Eq. (5) into Eq. (13).

III. Observability with set-valued output uncertainty

We will now define the set-valued observability measure to “control” the quality of estimation along a planned trajectory $x_{0:T}$. For the LTI system Eq. (1)-Eq. (2) with a Gaussian noise model, it is known that that estimation can be improved by optimizing over OG properties directly [26]. Generally the conditioning of the OG must be improved so that the estimation is robust and state is unique under measurement errors. For set-valued measurements, we build a similar setup. We first examine the notion of *distinguishability* that defines observability for a general class of nonlinear systems as defined it [35], to form the basis of our set-based definitions.

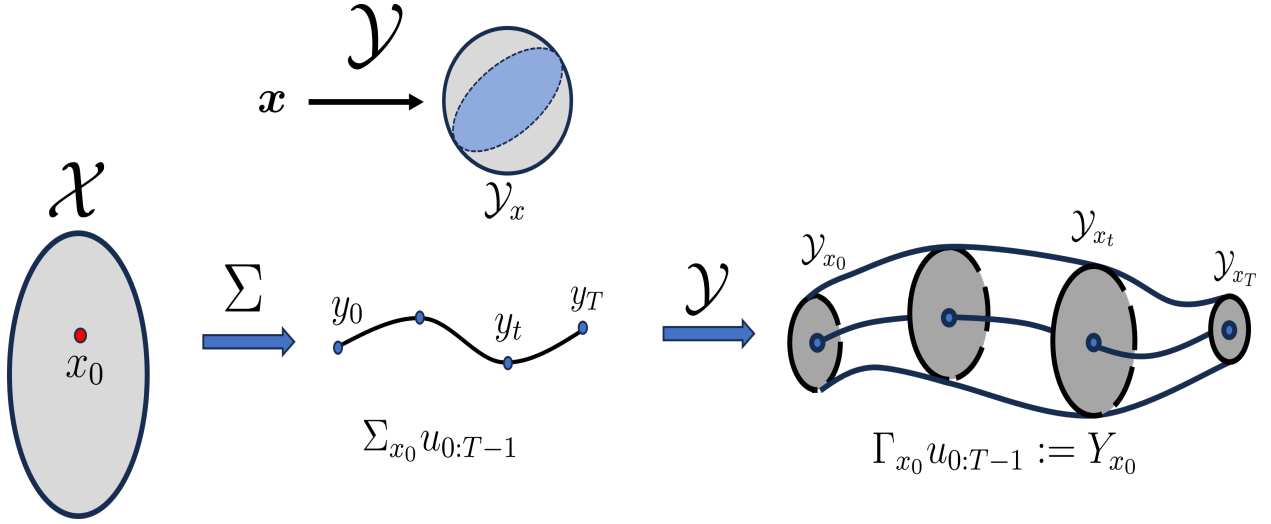


Fig. 1 The figure illustrates maps defined in §III. The map shown on top is \mathcal{Y} defined the output uncertainty at state x . The uncertainty shown in blue dashed ellipsoid is \mathcal{Y}_x and the maximum size $\Lambda(\mathcal{Y}_x)$ is shown by grey sphere around \mathcal{Y}_x .

On the bottom, the figure shows output sets generated by initial conditions $x_0 \in \mathcal{X}$. The map Σ generates a point-wise output trajectory for input sequence $u_{0:T-1}$. The uncertainty function \mathcal{Y} converts point-wise trajectory to a tube. We define the output tube map as $\Gamma = \mathcal{Y} \circ \Sigma$

Consider the system Eq. (1)-Eq. (2) with a given initial condition $\bar{x}_0 \in \mathcal{X}$ and input sequence $u_{0:T}$. For a given \bar{x}_0 , define the map from the input sequence to output sequence as $\Sigma_{\bar{x}_0} : (u_{0:T}) \rightarrow (y_{0:T})$. In this context, we say that state x_0 is *indistinguishable* from any other state $x_0 \in \mathcal{X}$ if for every admissible input sequence, we have $\Sigma_{\bar{x}_0}(u_{0:T}) = \Sigma_{x_0}(u_{0:T})$. The map Σ is said to be observable at \bar{x}_0 if, \bar{x}_0 is distinguishable. *Distinguishability*, means that for any input sequence and $\bar{x}_0 \in \mathcal{X}$, $\Sigma_{\bar{x}_0}(u_{0:T}) \neq \Sigma_{x_0}(u_{0:T})$.

Now in our context, for set-valued output maps, we need a notion of *distinguishability*. We use Assumption II.1 to say that given any two *distinct* states $\bar{x}, x \in \mathcal{X}$ the corresponding output sets $\mathcal{Y}_{\bar{x}}$ and \mathcal{Y}_x are “separated,” written as $\mathcal{Y}_{\bar{x}} \neq \mathcal{Y}_x$, when $d_s(\mathcal{Y}_{\bar{x}}, \mathcal{Y}_x) \neq 0$. The set-valued output sequence can be characterized by applying the point-to-set map \mathcal{Y} to Σ , giving us the map Γ from initial condition x_0 to output “cylinder”(output tube) for an input sequence $u_{0:T-1}$. The mapping is illustrated in Fig. 1. This output trajectory in the form of a cylinder as $\Gamma_{\bar{x}}(u_{0:T-1}) = \mathcal{Y}_{\bar{x}} \circ \Sigma_{\bar{x}}(u_{0:T-1})$. As such, Γ maps the initial condition and input sequence pair to a set valued output tube. We will denote the output tube by $\Gamma_{\bar{x}_0}(u_{0:T-1}) = \{\mathcal{Y}_{\bar{x}_0}, \dots, \mathcal{Y}_{\bar{x}_T}\}$, a sequence of set-valued elements also denoted by $Y_{\bar{x}_0:T}$.

$$x_0 \xrightarrow{\Sigma(\cdot, u_{0:T-1})} \Sigma_{x_0} u_{0:T-1} \xrightarrow{\mathcal{Y}} \Gamma_{x_0} u_{0:T-1} = \{\mathcal{Y}_{x_0}, \mathcal{Y}_{x_1}, \dots, \mathcal{Y}_{x_T}\} := Y_{x_0:T} \quad (15)$$

$$x_0 \xrightarrow{\Gamma(\cdot, u_{0:T-1})} Y_{x_0:T} \quad (16)$$

As defined in Eq. (16), the mapping Γ , parametrized by input sequence $u_{0:T-1}$ maps x_0 to output tube $Y_{x_0:T}$. We can now define a notion of observability for this scenario in terms of a condition on Γ for one-to-one mapping from \bar{x}_0 to the output tube of length T . Note that we will subsequently drop $u_{0:T-1}$ from the Γ notation to say that output map itself changes as $u_{0:T-1}$ does.

Definition III.1 *The system with set-valued output is said to be finite horizon weakly observable if for all $x \in U(\bar{x}_0)$ and input sequences,*

$$d_{\Gamma}(Y_{\bar{x}_0:T}, Y_{x_0:T}) = \sum_{t=0}^T d_s(\mathcal{Y}_{\bar{x}_t}, \mathcal{Y}_{x_t}) > 0 \implies d(\bar{x}_0, x_0) > 0, \quad (17)$$

for some $T > 0$; here $d_{\Gamma}(\cdot, \cdot)$ is the distance metric defined on output tubes.

The term *weakly*, suggests that the corresponding conditions are valid for \bar{x}_0 , and not for all $x \in \mathbb{X}$. This definition ensures that for finite horizon observability ($T > 0$), output tube generated by x_0 is distinct from those generated by neighboring initial states. The Fig. 2 illustrates an unobservable and a observable mapping from a initial condition in the set based setting. Here the finiteness of trajectory is necessary as the application requires a finite horizon solution depending on the task. A notion of short time observability has been used before for trajectory generation in deterministic output case by Alaeddini, Morgansen and Mesbahi [37].

Note that from Definition:III.1, we observe that horizon time for distinguishing initial conditions, e.g., T , may need to be arbitrarily large. This is not suitable for finite horizon optimal control problem, where for a fixed horizon $T' < T$ the system may become unobservable at \bar{x}_0 . Therefore observability condition needs to be imposed for a fixed T , where any initial condition $x_0 \notin B_{\delta}(\bar{x}_0)$ is distinguishable from \bar{x}_0 . Here $B_{\delta}(\bar{x}_0)$ is a ball around \bar{x}_0 . To define the observability metric we will pick a horizon $T > 0$ such that $\delta > 0$ is arbitrarily small. Now that a notion of observability has been established, we can design a state observer for the system Eq. (1-2). We will first define a notion for conditioning for observer design suitable for our set-valued analysis.

Degree of Observability

We can now define a inverse map from space of output tubes to a space of feasible initial state vectors, i.e., $\Gamma^{-1} : Y \rightarrow X$. If such an inverse set map exists such that for every Y_x there exists an initial condition x , then conditions for finite horizon observability have been met. It is important to note here that Γ^{-1} represents the estimator map as it takes measurement sequence space to the state vector.

Now, we examine the degree of observability using a regularity metric on sets [38–40].

Definition III.2 *(Inverse mapping and Metric Regularity) Consider two metric spaces (X, d) and (Y, d_{Γ}) and a set-valued mapping $\Gamma : X \rightarrow Y$. Then Γ is metrically regular at $\bar{x} \in X$ and $Y_{\bar{x}} \in Y$ if there exists constant $c > 0$ such*

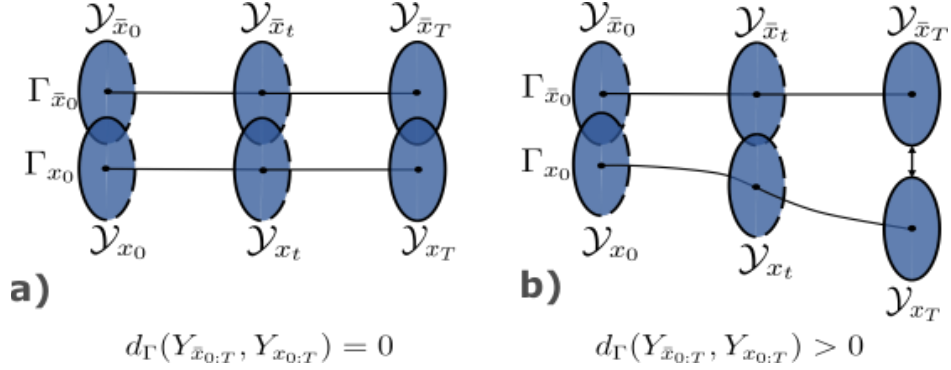


Fig. 2 We show an illustration of observability criterion for set-valued mappings. The figures show discrete slices of output tubes at times $0, t, T$. We show output tube for initial condition \bar{x}_0 and x for the map Γ with same input sequence $u_{0:T-1}$.

a) The case where output tubes generated from \bar{x}_0 and x_0 do not separate as shown by the figure, and $d_{\Gamma}(Y_{\bar{x}_0:T}, Y_{x_0:T}) = 0$. Thus \bar{x}_0 is not observable.

b) The case where output tubes generated from \bar{x}_0 and x_0 eventually separate, and $d_{\Gamma}(Y_{\bar{x}_0:T}, Y_{x_0:T}) > 0$. Thus \bar{x}_0 is observable.

that:

$$d(x, \Gamma^{-1}(Y_z)) \leq c d_{\Gamma}(Y, \Gamma(z)) \quad \forall (x, y) \text{ close to } (\bar{x}, \bar{y}), \quad (18)$$

where $\Gamma^{-1}(Y_z) = \{z \in X | y \in Y\}$. The distance metrics $d()$ and $d_{\Gamma}()$ are defined on sets and tubes respectively, and "close to" means for a small enough neighborhood.

The above definition characterizes the regularity of the map Γ^{-1} . The quantity $c > 0$ is system dependent and fixed for an LTI system.

From Eq. (18), we can see that a perturbation in the output tube is lower bounded by the tolerance on the state. For state estimation to be more robust, we want the state x tolerance $B_{\epsilon}(x)$ to remain small as perturbations in output tube increase. As defined previously $c > 0$ is constant and Γ is dependent on $u_{0:T-1}$ for LTI system Eq. (1)-(2). Hence in order to find a output robust map we must select the correct input sequence.

Lastly, given the tolerance $B_{\epsilon}(\bar{x}_0)$, we want \bar{x}_0 to be ϵ -distinguishable and highly robust to perturbations in tubes. Therefore, for any perturbed state $x_0 \in \mathcal{A} = \{x_0 | x_0 \notin B_{\epsilon}(\bar{x}_0)\}$, the worst-case perturbation in the output tube must be maximized. As such, we define the quantity for *degree of observability*[†] measuring the worst case perturbation in output when state has been perturbed:

[†]The notion of *degree of observability* comes from the definition of *modulus of regularity* [40] defined for the inverse map in Definition III.2. This notion of regularity is often used to analyze perturbations on set-valued maps.

$$\begin{aligned}
D_O(Y_{\bar{x}_{0:T}}) &= \inf_{x \in \mathcal{A}} d_\Gamma(Y_{\bar{x}_{0:T}}, Y_{x_{0:T}}) \\
&= \inf_{x \in \mathcal{A}} \sum_{t=0}^T d_s(\mathcal{Y}_{\bar{x}_t}, \mathcal{Y}_{x_t})
\end{aligned} \tag{19}$$

where,

$$\mathcal{A} = \{x \mid \|x - x_0\| > \epsilon\}. \tag{20}$$

We will use the notation $D_O(Y_{x_{0:T}})$ to denote degree of observability for a trajectory generated from x_0 with input sequence $u_{0:T}$. Maximizing $D_O(Y_{x_{0:T}})$ with respect to Γ , will decrease the sensitivity of estimator to large perturbations in measurements. Optimizing over Γ in this context corresponds to searching over output sequences $Y_{\bar{x}_{0:T}}$ that is a function of state sequence $\bar{x}_{0:T}$. Here if \bar{x}_0 and system parameters are given, then $\bar{x}_{0:T}$ is a linear function of $u_{0:T-1}$. Thus in the next section, we will build the setup for this problem of selecting input sequences to maximize observability.

IV. Improving observability over discrete time trajectories

As we have seen, the nominal output map Γ_{x_0} is a function of input sequence $u_{0:T}$ and its corresponding D_O is computed by evaluating trajectories in the region around a nominal trajectory with the same input sequence. We define this nominal trajectory with state input-pair \bar{x}_t, \bar{u}_t for the system Eq. (1)-(2).

In order to compute the perturbed trajectories, we define the perturbed dynamics as:

$$\begin{aligned}
\delta x_{t+1} &= A\delta x_t + B\delta u_t \\
\delta y_t &= C\delta x_t
\end{aligned}$$

where $\delta x_t = x_t - \bar{x}_t$, $\delta u_t = u_t - \bar{u}_t$ and $\delta y_t = y_t - \bar{y}_t$ are the deviations from nominal states, inputs and outputs at time $t \in [0, T-1]$. We can now compute a lower bound on discrete time degree of observability defined in Eq. 19. Here x_t is the trajectory generated by sampling x_0 from \mathcal{A} and propagating the dynamics with input sequence $u_t = \bar{u}_t$. If for all such x_0 , we have $d_\Gamma(Y_{\bar{x}_{0:T}}, Y_{x_{0:T}}) > 0$, then x_0 is finite horizon weakly observable. Hence, we compute the lower bound

by using Eq. (14) in Eq. (19), i.e.,

$$\begin{aligned}
D_{\mathcal{O}}(Y_{\bar{x}_{0:T}}) &\geq \inf_{x_0 \in \mathcal{A}} \sum_{t=0}^T \{ \|\bar{y}_t - y_t\| - \Lambda(\mathcal{Y}_{\bar{x}_t}) - \Lambda(\mathcal{Y}_{x_t}) \} \\
&\geq \sum_{t=0}^T \inf_{x_t \in \mathcal{A}} \{ \|\delta y_t\| - \Lambda(\mathcal{Y}_{\bar{x}_t}) - \Lambda(\mathcal{Y}_{x_t}) \} \\
&\geq \sum_{t=0}^T \inf_{x_t \in \mathcal{A}} \{ \|C\delta x_t\| - \Lambda(\mathcal{Y}_{\bar{x}_t}) - \Lambda(\mathcal{Y}_{x_t}) - L(\bar{x}_t)\|\delta x_t\| \} \\
&\geq \sum_{t=0}^T \inf_{x_t \in \mathcal{A}} \{ \|C\delta x_t\| - 2\Lambda(\mathcal{Y}_{\bar{x}_t}) - L(\bar{x}_t)\|\delta x_t\| \} \\
&\geq \sum_{t=0}^T \inf_{x_t \in \mathcal{A}} \{ \|CA^t\delta x_0\| - \|A^t\delta x_0\|L(\bar{x}_t) - 2\Lambda(\mathcal{Y}_{\bar{x}_t}) \} \tag{21} \\
&\geq \sum_{t=0}^T \left\{ \underbrace{\sigma_{\min}(CA^t)\epsilon}_{T1} - \underbrace{\sigma_{\max}(A^t)\epsilon L(\bar{x}_t) - 2\Lambda(\mathcal{Y}_{\bar{x}_t})}_{T2} \right\} \tag{22} \\
&:= D_{\mathcal{O}}^l(Y_{\bar{x}_{0:T}}),
\end{aligned}$$

where σ_{\max} and σ_{\min} are the largest and smallest singular values of their respective matrix arguments.

In order to impose the observability constraint, we set the lower bound as defined in Eq. (22) to be positive. Thus the parameter ϵ is selected such that for some positive $t \leq T$ we have the LHS of Eq. (22) as positive. If epsilon is selected such that lower bound of degree of observability is positive then, the separation term $T1$ and the uncertainty term $T2$ are independent of each other. Moreover the separation term $T1$ is not a function of the state x_t under the LTI assumption. Here we want $T1$ to be bounded, as the optimization problem involves maximizing this lower bound. Moreover if A is not Schur stable then $T1$ can be large for finite horizon problems and scaling for observability augmented costs becomes an issue. The term $T2$ which maps how uncertainty grows over the trajectory also needs to be bounded as with unbounded uncertainty, separability of trajectories and consequently observability becomes infeasible. Therefore we require Assumption (II.1) for uniform boundedness. The term $D_{\mathcal{O}}^l$ is now well defined. Note that in Eq. (14), we defined the distance to be non-negative. This also applies to $D_{\mathcal{O}}^l$. For observability though, we need this quantity to be positive, and by selecting large enough ϵ we can see from Eq. (14) that $D_{\mathcal{O}}^l > 0$. So for optimization problem we will pose shortly, ϵ will act as a tuning parameter that must be selected large enough for $D_{\mathcal{O}}^l$ to be positive.

The lower bound $D_{\mathcal{O}}^l(Y_{\bar{x}_{0:T}})$ on degree of observability is now only a function of state trajectory $x_{0:T}$. Combining all constraints we obtain a system with set-valued outputs which we define as observability-regular.

Definition IV.1 *The system Eq. (1)-(2) with set-valued outputs defined in Eq. (4) is observability-regular if Assumption II.1 holds and the system is finite horizon weakly observable.*

We will now state the main theorem for the observability measure.

Theorem IV.1 *Given a system with a finitely observable state \bar{x}_0 , the lower bound on the degree of observability is a concave function with respect to the state sequence $x_{0:T}$ if the output maps are observability-regular.*

Proof: Given x_0 and an observability-regular uncertainty mapping, we can compute the lower bound on the degree of observability as given by Eq. (22). Here Λ , and consequently $L(\bar{x})$, are convex. Thus Eq. (22) is a summation of concave functions and as such, concave. \square

Note that we structured the above proof on the condition that the uncertainty map is convex with respect to the state or has an upper-bounding envelope that is convex.

Now we can use this metric as a cost function in a optimal trajectory design problem. The solution to maximizing this metric for a given system is a state sequence that maximizes observability. Note that as we have noted earlier, this solution could lead to a solution that is unstable for an infinite horizon problem. For the finite horizon setting, maximizing this metric will lead to a trajectory that seeks optimal state estimation, but in applications, this trajectory might conflict with task completion such as reaching a desired final state. Therefore an estimation-aware optimization problem is presented as tool to generate a deviated trajectory to some nominal trajectory that achieves the desired task. Here the observability metric can be maximized under a constraint that limits deviation from the original nominal trajectory. Alternatively, since the observability metric is concave, we can add its negation to a trajectory design cost function with a regularization term. These two approaches demonstrate the application of the proposed set-valued observability metric to distinct trajectory design problems. We will now present the two approaches with representative applications.

V. Finite Horizon Estimation-Aware Trajectory Planning

We now need to find an estimation-aware trajectory in the neighborhood of nominal trajectory (\bar{x}, \bar{u}) , such that the degree of observability is maximized. To achieve this we design a convex optimization problem to minimize the negative of the concave function that is the lower bound on degree of observability. Since we are considering dynamical systems with states driven by inputs, we can write the optimization problem to find the input sequence that maximizes the degree of observability.

A. Maximizing observability for a nominal trajectory

We consider a two dimensional double integrator agent with position only measurements,

$$\begin{aligned} x^+ &= Ax + Bu, \\ y &= Cx + \varepsilon_x; \quad y \sim U\{\Lambda(\mathcal{Y}_x)\}. \end{aligned}$$

For this double integrator system the measurements represented by samples drawn uniformly from a set around Cx . The output set is defined as $\Lambda(\mathcal{Y}_x) = Cx + K\|Cx - y_s\|_2^2 + r_0$, where y_s is a light source position and r_0 is size of residual error. This is a state-dependent sensor showing light-intensity dependence of a sensor. The uncertainty size grows convexly away from light-source. The output map is *observability-regular* and follows Theorem IV.1 and therefore the degree of observability can be maximized. The estimation aware trajectory is an exploration strategy subject to deviation from a nominal LQR trajectory for a fixed initial condition. Therefore the optimization problem are designed for deviation variables, $\eta = x' - \bar{x}$ and $\xi = u' - \bar{u}$, where \bar{x}, \bar{u} are the nominal trajectory variables and x', u' represent the estimation-aware trajectory. Mission constraints are added to limit exploration with respect to the nominal trajectory as the primary mission task is to reach the desired final state. The optimal control problem is now defined as:

$$\begin{aligned}
\min_{\xi_0: \xi_{N-1}} \quad & -D_O^l(Y_{\bar{x}_0:T}) \\
\text{s.t.} \quad & \eta_{k+1} = A\eta_k + B\xi_k \quad \text{for all } k \in [0, N], \\
& \|\eta_t\| \leq \gamma \quad \text{for all } k \in [0, N], \\
& \eta_N = 0.
\end{aligned} \tag{23}$$

We present this optimization problem as a strategy to "explore" the state space for favorable neighboring and more observable trajectories such that initial condition and final state constraints are the same as original problem. Exploration in this context is application dependent and must be interpreted and utilized given the energy usage constraints. We add the exploration constraint term γ , placing a bound on the deviation from the nominal trajectory. The solutions for this problem setup are demonstrated in Fig. 3.

We used the light dependent sensor model in this example to show how to pose the optimization problem for state-dependent sensors. For this case, we now design a controller to follow each of the designed offline trajectories; a generic Luenberger observer is designed such that the measurement error converges. We then analyze the performance of the observer along the nominal and the estimation aware trajectory as shown in Fig. 3.

B. Observability based trajectory design for satellite rendezvous

We now focus on the trajectory generation problem for optimizing state estimation for a target tracking operation. Here the degree of observability metric is used as an augmented term in a finite horizon optimal trajectory problem. The underlying model for this setup is defined by relative dynamics between an Ego and an uncooperative Target satellite. A camera on the Ego satellite is used to capture Target images and an ML algorithm estimates the pose (position and orientation) of the uncooperative Target spacecraft relative to the Ego. We use an ML algorithm that identifies relative pose of the Target shown in an image taken from the Ego spacecraft. The implementation along with testing and

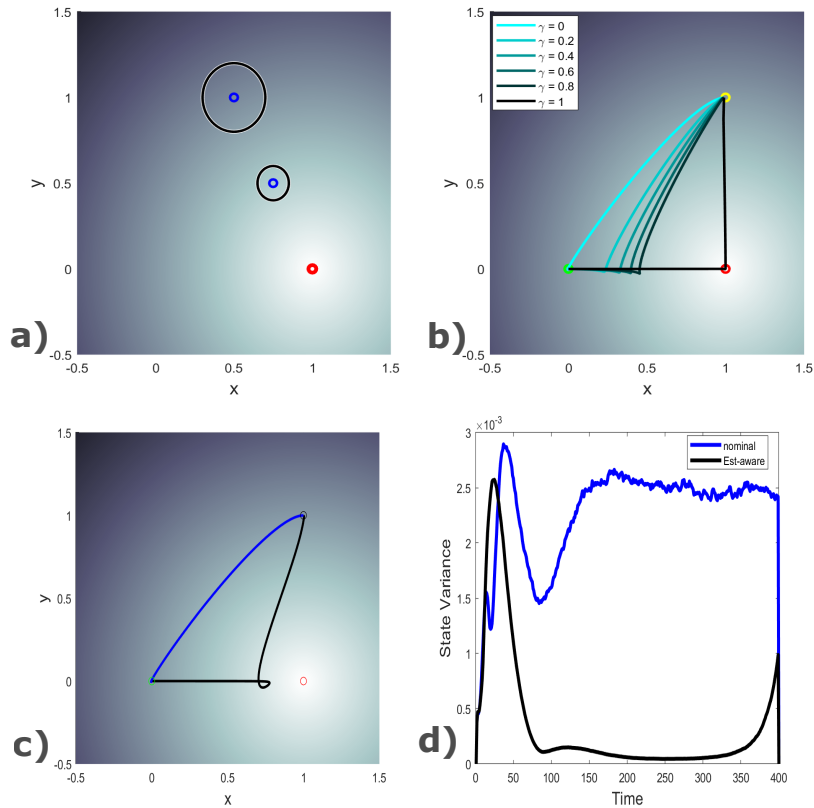


Fig. 3 The figure shows trajectory design for a double integrator system.

a) The red dots marks the light source. The output uncertainty grows radially outward from the light source. The circles in black represent the uncertainty around the outputs shown in blue.

b) The figure shows results of optimization problem. The estimation-aware trajectories have been generated using different exploration parameters γ as shown.

c) Sample of nominal and estimation-aware trajectories

d) State estimation performance while following both the trajectories shown on the left. The state estimation variance as converged after $N=10,000$ iterations over both the trajectories.

validation procedure for this algorithm has been shown in [41]. Using a photorealistic simulation engine we test the estimator under physically realistic lighting conditions. We observe that the estimation accuracy for relative Target pose, is a function of *illumination angle*, that is dependent on the Ego state. The illumination angle describes the difference between light incidence ray from the sun to the Target and the relative position vector between Ego and Target. The smaller the illumination angle, higher is the estimation accuracy. We estimate the upper bound on the error for the pose estimation with respect to the illumination angle using data gathered from our simulation engine in a validation routine. We then approximate the enveloping convex function that places an upper bound on the error with respect to the Ego state. The enveloping function is used as the convex map that defines the upper bound on the size of the uncertainty set. Now we have a system that satisfies conditions for Theorem IV.1, where the lower bound on the degree of observability is concave. As such, we can augment this function to a trajectory design optimization problem for the

satellite rendezvous operation. We use a modular simulation engine for visualization, data-gathering and validation as described in the Appendix.

The design problem is now formalized such that Ego spacecraft approaches the target with some initial separation and velocity relative to the Target. The Ego spacecraft is required to approach the Target while keeping out of a zone of 5 meters from the Target. The trajectory objective is designed such that quadratic terms add penalty to the relative Ego approach error and fuel consumption. The observability metric is added to the cost with a regularization term used as a tuning parameter. The optimization problem is thereby defined as follows:

$$\min_{u^{k_0:N-1}} J \quad (24)$$

$$x_{k+1} = x_k + f(x_k, u_k) \quad \forall k = 0, \dots, N \quad \text{Discretized relative dynamics} \quad (25)$$

$$\|x_k\| \geq d \quad \text{Keep-out zone} \quad (26)$$

$$u_k \sim \mathcal{U}_O, \quad x_k \sim \mathcal{X} \quad \text{State and action constraints} \quad (27)$$

where,

$$J = -\lambda_{\text{obs}} D^l_{\mathcal{O}}(Y_{\bar{x}_{0:T}}) + \sum_{k=0}^N l(x_k, u_k), \quad \lambda_{\text{obs}} > 0.$$

Here the regularization term λ_{obs} parametrizes the permissible deviation from the nominal trajectory. The objective function J is designed to be convex as $l(x_k, u_k) = x_k^T Q x_k + u_k^T R u_k$ and $(-D^l_{\mathcal{O}})$ are both convex. The discretized dynamics in this setting are linear as defined in Eq. (28 - 30). The keep-out zone constraints shown here are non-convex and therefore the optimization problem is non-convex in general. To search for a solution to this estimation-aware problem we use the successive convexification algorithm [42]. Here the non-convex problem is solved by iteratively solving convex sub-problems generated by linearizing the constraints and dynamics around a trust region. Note that without the non-convex constraint, the problem is convex for linear dynamics and we could use a convex solver to generate the guidance solution similar to the previous problem. An important aspect to here is that the successive convexification problem relies on the fact that sub-problems are convex in a trust region around the current iteration of the trajectory. In this case we must ensure that if the uncertainty size function is not convex globally it should at least be convex over the trust region. The regularization term $\lambda_{\text{obs}} > 0$, we use in the cost function is a tuning parameter that determines how much exploration we want to permit for the estimation aware trajectory.

The solution to this optimal control problem Eq. (24), is shown in Fig. 4. As such, the propose solution strategy obtains the estimation aware trajectory such that the Ego camera points to the Target with optimum illumination angle. We discuss further implementation details for this example in the Appendix and provide simulation results on Github[‡].

[‡]Additional simulation video and implementation details: https://github.com/Rainlabuw/Obs_aware_opt.git

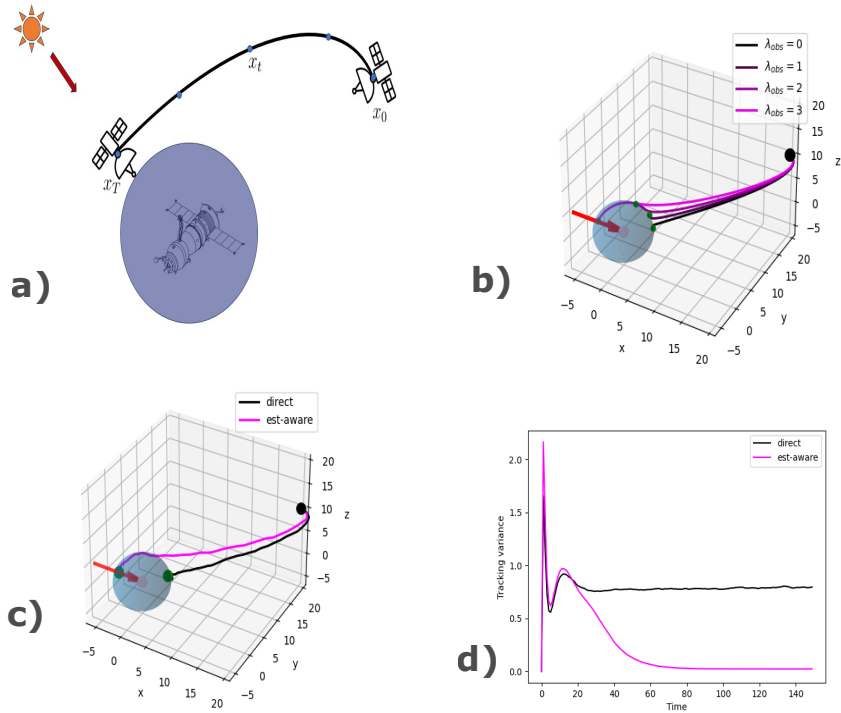


Fig. 4 The figure shows the estimation-aware trajectory generation for Ego-Target Rendezvous problem.

a) A representation of the Rendezvous problem where the Ego spacecraft starting at initial condition x_0 must rendezvous with the uncontrolled Target spacecraft while staying away from the keep-out zone shown in blue. The illumination angle as shown in the figure is known through a sun-sensor.

b) The Ego spacecraft starts at the initial spot shown in black, and reaches the goal position shown in green. We show the trajectories generated as a function of observability regularization term λ_{obs} . The most observable trajectory converges to a final position where illumination vector shown in red is parallel to the camera angle of the Ego spacecraft.

c) Trajectory follower algorithm implemented on both the nominal and the estimation aware trajectories with output uncertainties.

d) Estimation performance analysis for both trajectories over $N=50,000$ iterations.

VI. Conclusions

In this paper, we have presented an observability-based metric for set-valued and state dependent output maps. The proposed framework can be used to design estimation aware trajectories for set-valued uncertainty measurements. In particular, we require that the output uncertainty map must be convex in its size with respect to state or an enveloping convex function must be determined using a validation step to find an upper bound on uncertainty. We show that if the output maps are *observability-regular*, then we can define a lower bound on the *degree of observability*. Under reasonable assumptions on the state dependency of the uncertainty set, this lower bound is a concave function. We then proceeded to show that an optimization problem can be defined to maximize the degree of observability to generate an estimation aware trajectory. As such, a state observer designed for this system generates optimal state estimation along this estimation-aware trajectory.

We demonstrate that our observability metric can be used as a cost function term in trajectory design problems. We present a case study where an ML based state estimator by an Ego spacecraft is used to track uncooperative Target satellite. We use our procedure to constraint the estimator as a state-dependent set-valued map. We show that the metric we designed can be used to generate a tracking trajectory for the Ego spacecraft where the estimation accuracy has been improved. Alternatively we also show a that given a nominal trajectory, an neighboring estimation-aware trajectory can be designed by solely maximizing the observability metric lower bound while imposing exploration constraints in the neighborhood of the nominal trajectory.

This proposed framework has been defined for linear systems as well as sequentially linearized dynamics of relevance for non linear systems. Moreover finite horizon observability for set-based outputs can be defined for nonlinear systems but concavity of degree of observability metric is not guaranteed for general class of systems. We also believe that the proposed method is a useful tool to design offline estimation-aware trajectories if observability regular maps can be defined in neighborhood of a nominal trajectory. Further investigations into output uncertainties with non-ellipsoidal bounds would be a natural extension to this work.

Acknowledgments

The authors thank their various discussions on estimation-aware trajectory design with Spencer Kraisler, Shahriar Talebi, Beniamino Pozzan, Saptarshi Bandyopadhyay, Amir Rahmani, and Nick Andrews. The research of the authors has been supported by NSF grant ECCS-2149470 and AFOSR grant FA9550-20-1-0053.

VII. Appendix

Here we gather the complementary background pertaining to the main results presented in this work.

A. System Dynamics

The relative (translational) dynamics for the Ego spacecraft are given in the Hill's frame of Target. Specifically, the Clohessy–Wiltshire equations [43] are used to define the dynamics for position (x, y, z) (coordinates in the Hill's frame) and velocity $(\dot{x}, \dot{y}, \dot{z})$ as,

$$\ddot{x} = 3n^2x + 2n\dot{y} + u_x, \quad (28)$$

$$\ddot{y} = -2n\dot{x} + u_y, \quad (29)$$

$$\ddot{z} = -n^2z + u_z, \quad (30)$$

where n denotes the mean motion of Target spacecraft circular orbit and u 's are the control inputs in each corresponding axis. Now we define the position and velocity vectors as $p = [x, y, z]^T \in \mathbb{R}^3$ and $v = [\dot{x}, \dot{y}, \dot{z}]^T \in \mathbb{R}^3$. Redefine the state

vector as $x = [p^\top, v^\top]^\top \in \mathbb{R}^6$ and inputs as $u = [u_x, u_y, u_z]^\top \in \mathbb{R}^3$. The problem defined in Eq. (24) can now be solved using the discretized linear dynamics for the system defined in Eq. (28)-(30).

B. Simulation setup

We developed a closed-loop end-to-end pipeline that simulates high fidelity spacecraft dynamics and produces high resolution images for ML-based state estimator. The filtered state estimates are then used as feedback for tracking algorithms. The simulator is a modular setup where we can select appropriate astrodynamics simulators and estimators based on the application. The estimator primarily used here is a key-point-based pose estimation CNN that used segmentation to isolate the Target followed by a regression from image to key-point heat-maps. Detailed architecture of the CNN and integrated simulation pipeline has been described in our previous work [41].

Experiment Design

In order to provide robust guarantees, uniform error bounds must be provided for the perception map. We adopt a method similar to the procedure suggested by Dean *et al.* [44] but also introduce state-dependent bounds on the output.

We first simulate relative orbits of spacecraft in LEO in our simulation pipeline. The experiment design for the error modeling requires us to characterize error as a function of state dependent parameters. We now need to create the state-to-output uncertainty map as discussed in Eq. 4, and approximate its upper-bounding convex envelope. In this direction, we fix the Ego and Target relative position for each discretization point of the map. For each of these points, we discretely sample through all feasible Sun-angles observed under this scenario. Fig. 5 depicts one of these iterations where we set Target at the origin and arrow in black shows the relative Ego direction. The red arrows show a dense sampling of all the Sun-angles for this iteration. For each of these Sun-angles, we now randomize over all parameters that are not state dependent. Hence we randomize Earth positions, Target rotations and background noise and compute the norm error bound from all the outputs for the particular state and Sun-angle. This is repeated for all densely sampled Sun-angles and densely sampled states.

Relative state is sampled in increments of 5 meters starting from 10 meters to 45 meters, Sun-angles are sampled along longitudinal planes with 15 degree increments from zero to 180 degrees. Each Sun angle is repeated along a radial plane so that all views are accounted for. Lastly each iteration of the Sun angle is repeated for 50 random rotations so for each Sun angle we have 600 measurements. This generates the norm bound map as shown in the Fig. 5.[§]

In Fig. 5 we show the norm error bounds as a function of Sun-angle relative to Ego-Target relative direction. Each of the lines are an iteration of the state, i.e., fixed relative distance. This map shows that norm error bound grows monotonically as a function of Sun angle for this particular scenario. Given the validation dataset for error bound for

[§]We refer to [45] Corollary 7 (Hoeffding type inequality for norm-sub-Gaussian). Here we treat the uncertainty as a norm-bounded random variable which is a sub-Gaussian. The corollary states that summation of norm-bounded sub-Gaussians is bounded with some minimum probability that increases with the number of samples. We use the corollary to state that if bounded assumption on the norm of the random variable is valid, then the bound can be estimated with a known probability.

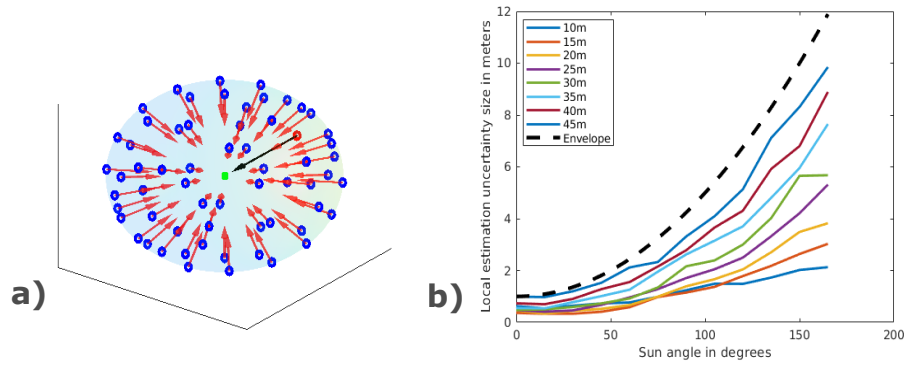


Fig. 5 The figure shows validation experiment design setup.

a) Representation of sampling strategy for validation step. Here black arrow shows Ego camera pointing at the Target in green when sun is directly behind the Ego spacecraft. Then by randomly placing the Ego on a sphere we get different target angles and background for each point with the red arrow. This is repeated for spheres of varying length.

b) The plot shows uncertainty size with respect to each iteration of relative distance represented by a sphere on the right. The envelope function is represented in dashed black line. The candidate class used for envelope function here is a quadratic function. Here we observe the state dependence of output uncertainty in tracking the target as a function of sun angle.

subject to Ego-state, we can compute the uncertainty radius upper bound using a quadratic envelope.

Our implementation setup and supplementary information are described on GitHub.[¶]

References

- [1] Malyuta, D., Reynolds, T. P., Szmuk, M., Lew, T., Bonalli, R., Pavone, M., and Açıkmeşe, B., “Convex Optimization for Trajectory Generation: A Tutorial on Generating Dynamically Feasible Trajectories Reliably and Efficiently,” *IEEE Control Systems Magazine*, Vol. 42, No. 5, 2022, pp. 40–113. <https://doi.org/10.1109/MCS.2022.3187542>.
- [2] Costante, G., Forster, C., Delmerico, J. A., Valigi, P., and Scaramuzza, D., “Perception-aware Path Planning,” *arXiv preprint arXiv:1605.04151*, Vol. abs/1605.04151, 2016. URL <https://doi.org/10.48550/arXiv.1605.04151>.
- [3] Kalman, R. E., “A New Approach to Linear Filtering and Prediction Problems,” *Transactions of the ASME—Journal of Basic Engineering*, Vol. 82, No. 1, 1960, pp. 35–45. <https://doi.org/10.1115/1.3662552>.
- [4] Gustafsson, F., “Particle Filter Theory and Practice with Positioning Applications,” *IEEE Aerospace and Electronic Systems Magazine*, Vol. 25, No. 7, 2010, pp. 53–82. <https://doi.org/10.1109/MAES.2010.5546308>.
- [5] Menegaz, H. M. T., Ishihara, J. Y., Borges, G. A., and Vargas, A. N., “A Systematization of The Unscented Kalman Filter Theory,” *IEEE Transactions on Automatic Control*, Vol. 60, No. 10, 2015, pp. 2583–2598. <https://doi.org/10.1109/TAC.2015.2404511>.
- [6] Jouin, M., Gouriveau, R., Hissel, D., Péra, M.-C., and Zerhouni, N., “Particle Filter-Based Prognostics: Review, Discussion and

[¶]https://github.com/Rainlabuw/Obs_aware_opt.git

- Perspectives,” *Mechanical Systems and Signal Processing*, Vol. 72-73, 2016, pp. 2–31. <https://doi.org/10.1016/j.ymssp.2015.11.008>.
- [7] Taghvaei, A., and Mehta, P. G., “An Optimal Transport Formulation of the Ensemble Kalman Filter,” *IEEE Transactions on Automatic Control*, Vol. 66, No. 7, 2021, pp. 3052–3067. <https://doi.org/10.1109/TAC.2020.3015410>.
- [8] Alaeddini, A., Morgansen, K. A., and Mesbahi, M., “Augmented State Feedback for Improving Observability of Linear Systems with Nonlinear Measurements,” *Systems & Control Letters*, Vol. 133, 2019, p. 104520. <https://doi.org/10.1016/j.sysconle.2019.104520>.
- [9] Murali, V., Spasojevic, I., Guerra, W., and Karaman, S., “Perception-aware trajectory generation for aggressive quadrotor flight using differential flatness,” *American Control Conference*, 2019, pp. 3936–3943. <https://doi.org/10.23919/ACC.2019.8814697>.
- [10] Blackmore, L., Rajamanoharan, S., and Williams, B. C., “Active Estimation for Jump Markov Linear Systems,” *IEEE Transactions on Automatic Control*, Vol. 53, No. 10, 2008, pp. 2223–2236. <https://doi.org/10.1109/TAC.2008.2006100>.
- [11] Zois, D.-S., and Mitra, U., “Active State Tracking With Sensing Costs: Analysis of Two-States and Methods for n -States,” *IEEE Transactions on Signal Processing*, Vol. 65, No. 11, 2017, pp. 2828–2843. <https://doi.org/10.1109/TSP.2017.2664049>.
- [12] Krishnamurthy, V., and Djonin, D. V., “Structured Threshold Policies for Dynamic Sensor Scheduling—A Partially Observed Markov Decision Process Approach,” *IEEE Transactions on Signal Processing*, Vol. 55, No. 10, 2007, pp. 4938–4957. <https://doi.org/10.1109/TSP.2007.897908>.
- [13] Zois, D.-S., Levorato, M., and Mitra, U., “Active Classification for POMDPs: A Kalman-Like State Estimator,” *IEEE Transactions on Signal Processing*, Vol. 62, No. 23, 2014, pp. 6209–6224. <https://doi.org/10.1109/TSP.2014.2362098>.
- [14] Flayac, E., Dahia, K., Hérisse, B., and Jean, F., “Nonlinear Fisher Particle Output Feedback Control and its Application to Terrain Aided Navigation,” *2017 IEEE 56th Annual Conference on Decision and Control (CDC)*, 2017, pp. 1566–1571. <https://doi.org/10.1109/CDC.2017.8263874>.
- [15] Kreutz, C., and Timmer, J., *Encyclopedia of Systems Biology*, Springer New York, New York, NY, 2013, Chaps. Optimal Experiment Design, Fisher Information, pp. 1576–1579. https://doi.org/10.1007/978-1-4419-9863-7_1222.
- [16] Fisher, R. A., “Theory of Statistical Estimation,” *Mathematical Proceedings of the Cambridge Philosophical Society*, Vol. 22, No. 5, 1925, p. 700–725. <https://doi.org/10.1017/S0305004100009580>.
- [17] Plastino, A. R., and Plastino, A., “What’s the Big Idea? Cramér–Rao Inequality and Rao Distance,” *Significance*, Vol. 17, No. 4, 2020, pp. 39–39. <https://doi.org/10.1111/1740-9713.01425>.
- [18] Rao, C. R., *Breakthroughs in Statistics: Foundations and Basic Theory*, Springer New York, New York, NY, 1992, Chap. Information and the Accuracy Attainable in the Estimation of Statistical Parameters, pp. 235–247. https://doi.org/10.1007/978-1-4612-0919-5_16.

- [19] Singh, A., and Hahn, J., “Determining Optimal Sensor Locations for State and Parameter Estimation for Stable Nonlinear Systems,” *Industrial and Engineering Chemistry Research*, Vol. 44, 2005. <https://doi.org/10.1021/ie040212v>.
- [20] Ober, R. J., “The Fisher Information Matrix for Linear Systems,” *Systems and Control Letters*, Vol. 47, No. 3, 2002, pp. 221–226. [https://doi.org/10.1016/S0167-6911\(02\)00190-1](https://doi.org/10.1016/S0167-6911(02)00190-1).
- [21] Wang, Z., Shen, X., and Zhu, Y., “Posterior Cramér-Rao Bounds for Nonlinear Dynamic System with Colored Noises,” *Journal of Systems Science and Complexity*, Vol. 32, No. 6, 2019, p. 1526–1543. <https://doi.org/10.1007/s11424-019-7310-5>.
- [22] Okamoto, K., and Tsiotras, P., “Optimal Stochastic Vehicle Path Planning Using Covariance Steering,” *IEEE Robotics and Automation Letters*, Vol. 4, No. 3, 2019, pp. 2276–2281. <https://doi.org/10.1109/LRA.2019.2901546>.
- [23] Rafieisakhaei, M., Chakravorty, S., and Kumar, P. R., “On the Use of the Observability Gramian for Partially Observed Robotic Path Planning Problems,” *2017 IEEE 56th Annual Conference on Decision and Control (CDC)*, 2017, pp. 1523–1528. <https://doi.org/10.1109/CDC.2017.8263868>.
- [24] Powel, N. D., and Morgansen, K. A., “Empirical Observability Gramian for Stochastic Observability of Nonlinear Systems,” *ArXiv*, Vol. abs/2006.07451, 2020. <https://doi.org/10.48550/arXiv.2006.07451>.
- [25] Avant, T., and Morgansen, K. A., “Observability Properties of Object Pose Estimation,” *2019 American Control Conference (ACC)*, 2019, pp. 5134–5140. <https://doi.org/10.23919/ACC.2019.8814791>.
- [26] Alaeddini, A., and Morgansen, K. A., “Trajectory Design for a Nonlinear System to Insure Observability,” *2014 European Control Conference (ECC)*, 2014, pp. 2520–2525. <https://doi.org/10.1109/ECC.2014.6862598>.
- [27] Boyinine, R., Sharma, R., and Brink, K., “Observability Based Path Planning for Multi-Agent Systems to Aid Relative Pose Estimation,” *2022 International Conference on Unmanned Aircraft Systems (ICUAS)*, 2022, pp. 912–921. <https://doi.org/10.1109/ICUAS54217.2022.9836a088>.
- [28] Glotzbach, T., Crasta, N., and Ament, C., “Observability Analyses and Trajectory Planning for Tracking of an Underwater Robot using Empirical Gramians,” *IFAC Proceedings Volumes*, Vol. 47, No. 3, 2014, pp. 4215–4221. <https://doi.org/10.3182/20140824-6-ZA-1003.01939>.
- [29] Krener, A. J., and Ide, K., “Measures of Unobservability,” *Proceedings of the 48th IEEE Conference on Decision and Control (CDC) held jointly with 2009 28th Chinese Control Conference*, 2009, pp. 6401–6406. <https://doi.org/10.1109/CDC.2009.5400067>.
- [30] Lall, S., Marsden, J. E., and Glavaški, S., “Empirical Model Reduction of Controlled Nonlinear Systems,” *IFAC Proceedings Volumes*, Vol. 32, No. 2, 1999, pp. 2598–2603. [https://doi.org/10.1016/S1474-6670\(17\)56442-3](https://doi.org/10.1016/S1474-6670(17)56442-3).
- [31] Tang, W., Wang, Z., Zhang, Q., and Shen, Y., “Set-Membership Estimation for Linear Time-Varying Descriptor Systems,” *Automatica*, Vol. 115, 2020, p. 108867. <https://doi.org/10.1016/j.automat.2020.108867>.

- [32] Tang, Y., Lasserre, J.-B., and Yang, H., “Uncertainty Quantification of Set-Membership Estimation in Control and Perception: Revisiting the Minimum Enclosing Ellipsoid,” *Proceedings of Machine Learning Research*, 2024. <https://doi.org/10.48550/arXiv.2311.15962>.
- [33] Ding, Y., Cong, Y., and Wang, X., “Set-Membership Filtering-Based Cooperative State Estimation for Multi-Agent Systems,” *2023 42nd Chinese Control Conference (CCC)*, 2023, pp. 5791–5796. <https://doi.org/10.23919/CCC58697.2023.10240662>.
- [34] Deole, A., Pozzan, B., and Mesbahi, M., “MPC-Based Estimation-Aware Trajectory Generation for Uncontrolled Satellite Pose Tracking,” *AIAA SCITECH 2024 Forum*, 2024. <https://doi.org/10.2514/6.2024-0947>.
- [35] Hermann, R., and Krener, A., “Nonlinear Controllability and Observability,” *IEEE Transactions on Automatic Control*, Vol. 22, No. 5, 1977, pp. 728–740. <https://doi.org/10.1109/TAC.1977.1101601>.
- [36] Roberts, A. W., and Varberg, D. E., “Another Proof that Convex Functions are Locally Lipschitz,” *The American Mathematical Monthly*, Vol. 81, No. 9, 1974, p. 1014–1016. <https://doi.org/10.1080/00029890.1974.11993721>.
- [37] Alaeddini, A., Morgansen, K. A., and Mesbahi, M., “Optimal Control with Limited Sensing via Empirical Gramians and Piecewise Linear Feedback,” *arXiv: Systems and Control*, 2016. <https://doi.org/10.48550/arXiv.1611.08056>.
- [38] Dontchev, A. L., and Hager, W. W., “An Inverse Mapping Theorem for Set-Valued Maps,” *Proceedings of the American Mathematical Society*, Vol. 121, No. 2, 1994, pp. 481–489.
- [39] Frankowska, H., and Quincampoix, M., “Hölder Metric Regularity of Set-Valued Maps,” *Mathematical Programming*, Vol. 132, No. 1–2, 2010, p. 333–354. <https://doi.org/10.1007/s10107-010-0401-7>.
- [40] Dontchev, A. L., and Lewis, A. S., “Perturbations and Metric Regularity,” *Set-Valued Analysis*, Vol. 13, No. 4, 2005, p. 417–438. <https://doi.org/10.1007/s11228-005-4404-0>.
- [41] Beckett, J., Seto, W., Deole, A., Bandyopadhyay, S., Rahimi, N., Talebi, S., Mesbahi, M., and Rahmani, A., “Robust Vision-based Multi-spacecraft Guidance Navigation and Control using CNN-based Pose Estimation,” *2022 IEEE Aerospace Conference (AERO)*, 2022, pp. 1–10. <https://doi.org/10.1109/AERO53065.2022.9843396>.
- [42] Mao, Y., Szmuk, M., Xu, X., and Açikmese, B., “Successive Convexification: A Superlinearly Convergent Algorithm for Non-convex Optimal Control Problems,” *arXiv: Optimization and Control*, 2018. <https://doi.org/10.48550/arXiv.1804.06539>.
- [43] Sparrow, G. W., and Price, D. B., *Derivation of Approximate Equations for Solving the Planar Rendezvous Problem*, National Aeronautics and Space Administration, District of Columbia, 1968.
- [44] Dean, S., Matni, N., Recht, B., and Ye, V., “Robust Guarantees for Perception-Based Control,” *Conference on Learning for Dynamics & Control*, 2019, p. 1. URL <https://api.semanticscholar.org/CorpusID:195833348>.
- [45] Jin, C., Netrapalli, P., Ge, R., Kakade, S. M., and Jordan, M. I., “A Short Note on Concentration Inequalities for Random Vectors with SubGaussian Norm,” *ArXiv*, Vol. abs/1902.03736, 2019.